Magnetoelectric Spectroscopy of Electronic Transitions in Antiferromagnetic Cr_2O_3

B. B. Krichevtsov, V. V. Pavlov, R. V. Pisarev, and V. N. Gridnev
Ioffe Physico-Technical Institute of the Russian Academy of Sciences, St. Petersburg 194021, Russia
(Received 22 January 1996)

Optical effects due to electric dipole–magnetic dipole interference were predicted for crystals which are noninvariant under space-inversion and time-reversal symmetry. We report measurements of the nonreciprocal rotation and ellipticity of light reflected from antiferromagnetic-magnetoelectric Cr_2O_3 in a spectral range from 1.6 to 2.5 eV, which comprises $^4A_2 \rightarrow {}^2E$, $^2T_1$, and $^4T_2$ transitions. An analysis provides new information about symmetries of excited states and shows that previous assignments of excitonic lines cannot be entirely reconciled with our data. [S0031-9007(96)00330-4]

PACS numbers: 78.20.Ls, 75.50.Ee, 75.80.+q

It is well known that the space-inversion symmetry ($\bar{1}$) breaking creates a large variety of optical phenomena, which are forbidden in centrosymmetric crystals. The well known example is the optical activity; see, e.g., [1]. From a microscopical point of view these effects arise due to the fact that matrix elements of odd and even (under space-inversion) operators between the same pairs of crystal states may be *simultaneously* nonzero. Thus, matrix elements of the electric dipole $\mathbf{d}_{nk}$ and the magnetic dipole $\mathbf{m}_{nk}$ (or electric quadrupole) moments between states $|n\rangle$ and $|k\rangle$ give rise to a contribution $g_{ij}^{(nk)}$ to the second-rank axial tensor g_{ij}, which describes a rotation of the polarization plane of light wave propagating through a crystal

$$g_{ij}^{(nk)} \sim \mathrm{Im} d_{kn}^i m_{nk}^j , \quad (1)$$

where i and j are Cartesian indices. The tensor g_{ij} is *time even* and, hence, may be nonzero in crystals both invariant and noninvariant under the time-reversal operation ($1'$). The *time-odd* axial property tensor α_{ij} may exist in crystals with the broken $\bar{1}$ and $1'$ symmetries [2]:

$$\alpha_{ij}^{(nk)} \sim \mathrm{Re} d_{kn}^i m_{nk}^j . \quad (2)$$

This tensor gives rise to the gyrotropic birefringence in transmission and to the nonreciprocal (NR) rotation of plane polarized light in reflection. First estimates of these effects gave values on the order of 10^{-8} rad [2] and thus were not encouraging for an experimental search. New microscopical theories reported quite recently [3–5] (see also [6]) showed that NR optical effects related to α_{ij} may be on the order of 10^{-4}–10^{-5} and, hence, they could be detectable using modern polarimetric techniques. Measurements of the NR rotation and ellipticity of reflected light were done only at one wavelength ($\lambda = 0.6328$ μm) in antiferromagnetic Cr_2O_3 [7] in which the magnetic symmetry allows the property tensor α_{ij}. Values on the order of 10^{-4}–10^{-5} rad were obtained for the rotation and ellipticity; however, they could be hardly regarded as proving or disproving theoretical estimates [3–5]. In fact, the coincidence might have been accidental, since, as we show below, the rotation and ellipticity change their magnitudes and signs when sweeping the frequency of light through the d-d absorption bands of Cr_2O_3.

We note in passing that an attempt to interpret the rotation in reflection in time-invariant crystal GaAs as a nonreciprocal effect [8] is completely inconsistent with the time-reversal symmetry of electromagnetic interactions. This interpretation was recently criticized in [9].

Taking into account (i) controversial estimates of the magnitude of the property tensor α_{ij}, (ii) its possible strong frequency dispersion in optical range, and (iii) its relation to a new kind of interference between electric dipole-magnetic dipole mechanisms which should lead to spectra different from those observed in absorption, we report in this Letter results on the first *spectroscopic* study of NR optical effects in reflection in Cr_2O_3, a material with well known crystallographic and magnetic structures. We show that observed effects are in agreement with recent estimates [3–5]. Our studies provide new information about the nature of electronic transitions and their splittings under the combined action of exchange and spin-orbit interaction.

The experimental setup is shown in Fig. 1. The light from a 150 W halogen-tungsten lamp S passes through a water filter F, a Glan polarizer GP, and a polarizing beam splitter BS. Then the light with polarization $\mathbf{E}_1$ passes through the modulator M and is focused by the lens L_4 on the surface of the sample in the optical cryostat. The reflected light goes back through the modulator M and passes the polarizing beam splitter BS. The light with polarization $\mathbf{E}_2 \perp \mathbf{E}_1$ is directed to the input slit of a grating monochromator. The intensity of light is measured on the first and the second harmonic of the operating frequency of polarization modulator.

When measuring the rotation, the Faraday cell was used as a polarization modulator (400 Hz). The measurements were carried out by a compensation method. For this purpose an electronic scheme generated in the Faraday

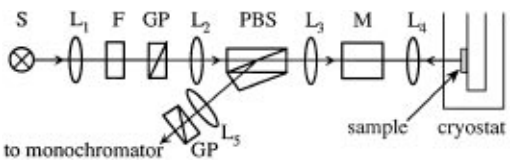

FIG. 1. Schematic of experimental setup.

 0031-9007/96/76(24)/4628(4)$10.00

cell the dc rotation of polarization plane of the same magnitude and of the opposite sign as compared to the rotation caused by reflection from a sample. The sensitivity was $\simeq 10^{-5}$ rad.

When measuring the ellipticity, which is proportional in our geometry to the circular dichroism in reflection, the photoelastic modulator was used. The ellipticity of reflected light was calculated as $\varepsilon = (\delta/4)I_1/I_2$, where I_1 and I_2 are the magnitudes of electrical signals on the first and second harmonics, respectively, of the operating frequency (32 kHz) of photoelastic modulator; $\delta = 0.08-0.12$ is the amplitude of ellipticity modulation. The sensitivity was $\simeq 10^{-5}$ rad.

Below the Néel temperature, $T_N = 307$ K, Cr_2O_3 has magnetic point group D_{3d} (D_3), which allows the magnetoelectric (ME) effect, i.e., nonzero tensor α_{ij}. C_3-axis-oriented platelike samples ($3 \times 3 \times 0.5$ mm) were prepared from boules of Cr_2O_3 grown by the Verneuil method. The crystals surface was polished by a diamond abrasive. For elimination of possible reciprocal effects measurements were performed for two single-domain antiferromagnetic states l^+ and l^-, which were produced by a magnetoelectric annealing procedure in a dc electric field $E = \pm 200$ V/mm and magnetic field $H = \pm 2$ kOe directed along the z axis. The annealing fields were switched off after cooling the sample and the measurements were performed without any external fields, i.e., the spontaneous effects were measured. The difference between measured values of the rotation and ellipticity in l^+ and l^- states is due to NR effects only [7,10].

The rotation and ellipticity were measured in the spectral range 1.6–2.5 eV with the resolution 2 meV in the temperature region 50–300 K. The measurements were carried out in geometry $\mathbf{k} \parallel z$ at normal reflection of light from the z plane of the crystal. The deviation from the normal incidence due to the focusing of light was $\simeq 10°$.

Figure 2 shows the spectral variations of NR effects at temperatures 274 and 90 K. At 90 K both the rotation and ellipticity reveal strong sharp lines of different signs in the spectral range 1.7–1.8 eV. The ellipticity in the region 1.9–2.3 eV shows two bands of different signs centered at 2.05 and 2.17 eV. The magnitudes of rotation and ellipticity at $E = 1.98$ eV ($\lambda = 0.63$ μm) are in good agreement with the data obtained in [7] by means of the laser polarimetric technique.

Figure 3 shows the spectra of NR ellipticity and rotation at $T = 90$ K in the spectral range 1.68–1.8 eV. The strongest line observed at $E = 1.704$ eV corresponds to the low-energy ^2E exciton [11–13]. Two weak lines of different signs in the region of ^2E excitons are placed at $E = 1.727$ and 1.732 eV. Three lines at 1.751, 1.758, and 1.763 eV originate in $^2T_1$ states.

The observed values of rotation θ and ellipticity ε are given by [2]

$$\theta + i\varepsilon = 2\alpha_\perp(1 + n_\perp)/(1 - n_\perp), \qquad (3)$$

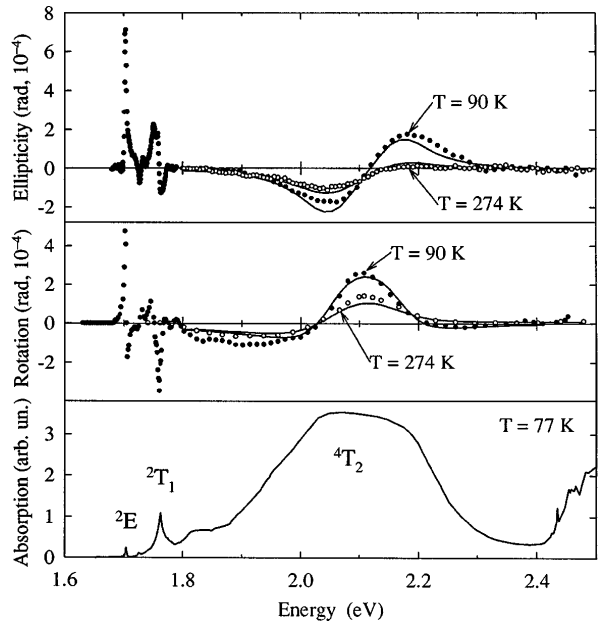

FIG. 2. Nonreciprocal ellipticity and rotation below T_N. No effects were observed above T_N. Solid lines are best fit calculations using a Lorentz-type oscillator model. The absorption spectrum is shown schematically using data from [15].

where $\alpha_\perp = \alpha_{xx}(\omega) = \alpha_{yy}(\omega)$ is the component of the ME tensor and $n_\perp^2 = \epsilon_{xx}(\omega) = \epsilon_{yy}(\omega)$. Because of a weakness of d-d transitions, the dispersion of $n_\perp(\omega)$ is small and, as seen from Eq. (3), the spectral dependence of the rotation and ellipticity is determined mainly by a frequency dependence of $\mathrm{Re}\alpha_\perp(\omega)$ and $\mathrm{Im}\alpha_\perp(\omega)$, respectively. When considering intraion d-d transitions we may use a noninteracting-ion model in which a

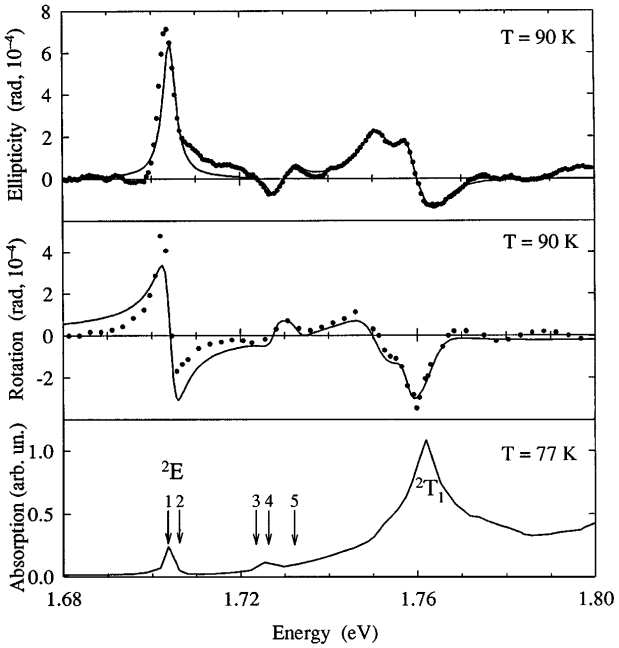

FIG. 3. Nonreciprocal ellipticity and rotation at 90 K in the region of spin-forbidden transitions $^4A_2$-^2E and $^4A_2$-$^2T_1$.

contribution of a single Cr^{3+} ion $\alpha_{ii}^{\rm ion}(\omega)$ to the tensor $\alpha_{ii}(\omega)$ is given by [1,2]

$$\alpha_{ii}^{\rm ion}(\omega) = \frac{4\pi}{\hbar}\sum_{k,n}\rho_k\left\{\frac{{\rm Re}\, d_{nk}^i m_{kn}^i}{\omega_{nk} + \omega + i\delta_{nk}} + \frac{{\rm Re}\, m_{kn}^i d_{nk}^i}{\omega_{nk} - \omega - i\delta_{nk}}\right\}, \quad (4)$$

where the sums run over all single-ion states; $\hbar\omega_{nk} = E_n - E_k$ is the energy difference between states n and k, δ_{nk} includes the effects of damping, and ρ_k is the occupation probability of the state k. As is seen from Eqs. (3) and (4), the frequency dependence of the rotation and ellipticity in the region of isolated transition has dispersion and absorptionlike forms, respectively. However, the quantities $\theta(\omega)$ and $\varepsilon(\omega)$ may behave differently when transitions to several states are overlaping [14].

Above T_N the tensor α_{ij} vanishes due to the time-reversal and parity symmetries. However, below T_N, due to the magnetic symmetry of Cr_2O_3 each Cr^{3+} ion brings exactly the same contribution $\alpha_{ii}^{\rm ion}(\omega)$ to the ME tensor [2], i.e., $\alpha_{ii}(\omega) = \mathcal{N}\alpha_{ii}^{\rm ion}(\omega)$, where $\mathcal{N} \simeq 4 \times 10^{22}$ cm^{-3} is the density of Cr^{3+} ions.

Note that in the optical range the ME tensor $\alpha_{ij}(\omega)$ arises as a result of a decomposition of the third-rank tensor $\gamma_{ijl}(\omega)$, which describes the first-order spatial dispersion, into the irreducible representations of the rotation group [2]. Another part of this decomposition, related to the quadrupole moments, does not contribute to the NR reflection under the normal incidence of light [7]. The diagonal components of $\alpha_{ii}(\omega)$ cannot be measured in transmission, but only in reflection experiments [2,7].

The optical absorption in Cr_2O_3 [15] is characterized by two wide absorption bands due to transitions from the ground term $^4A_2$ of the Cr^{3+} ion to the excited manifolds originated in the cubic crystal-field terms $^4T_2$ and $^4T_1$. Besides there are series of sharp lines associated with the spin-forbidden transitions to the terms ^2E, $^2T_1$, and $^2T_2$. The lines observed in rotation and ellipticity correspond in general to lines observed in absorption spectrum [15] shown schematically in Figs. 2 and 3, but in contrast to the absorption, NR effects may have different signs for different optical transitions.

First we discuss the spin-allowed transition $^4A_2 \rightarrow {}^4T_2$. As seen from Fig. 2 it is split into 2.051 and 2.169 eV bands. In order to explain this splitting we should consider the structure of $^4A_2$ and $^4T_2$ manifolds of states appearing under the action of the trigonal and the exchange fields as well as the spin-orbit interaction. The trigonal field splits the $^4T_2$ cubic term into two terms of the C_3 group: ^4A and ^4E with wave functions $|a, M_S\rangle$ and $|u_\pm, M_S\rangle$, where $M_S = \pm\frac{3}{2}, \pm\frac{1}{2}$. The exchange field splits states with different M_S and the spin-orbit interaction mixes states $|u_\pm, M_S\rangle$ and $|a, M_S \pm 1\rangle$. As a result we obtain two states to which the transitions from $|^4A_2 - \frac{3}{2}\rangle$ are allowed:

$$\Psi_1 = |u_+ - \tfrac{3}{2}\rangle + \beta|a - \tfrac{1}{2}\rangle, \quad (5)$$

$$\Psi_2 = |a - \tfrac{1}{2}\rangle - \beta^*|u_+ - \tfrac{3}{2}\rangle. \quad (6)$$

Here $\beta \sim \lambda_{\rm so}/\upsilon$, where $\lambda_{\rm so}$ is the spin-orbit coupling parameter and υ is the parameter of the trigonal splitting.

By using Eq. (4) it can be shown that transitions to the states (5) and (6) bring equal but opposite in sign contributions to $\alpha_\perp(\omega)$. The spin-orbit mixing of the $|^4A_2 - \frac{3}{2}\rangle$ state with the components of the $^4T_2$ multiplet modifies this simple relation between magnitudes of ^4E and ^4A bands. The energy separation of 2.051 and 2.169 eV bands somewhat exceeds the trigonal splitting obtained in absorption [15] that most probably is due to a combined action of the trigonal, exchange, and spin-orbit interactions on $^4A_2$ and $^4T_2$ manifolds. Thus, we qualitatively explain the behavior of $\alpha_\perp(\omega)$ in the region of $^4A_2 \rightarrow {}^4T_2$ transition. Note that in absorption the trigonal splitting of the $^4T_2$ term cannot be observed in axial polarization [16].

This consideration clearly demonstrates that the frequency dependence of the rotation and ellipticity is determined not only by a magnitude of $d_{kn}^i m_{nk}^j$, but also by its sign. This feature makes the NR rotation and ellipticity sensitive to the symmetry of electronic states. The value $d_{kn}^i m_{nk}^j$ has different signs for the transitions to the states (5) and (6), thus providing different signs of the ellipticities of 2.051 and 2.169 eV bands.

Now we turn to the spin-forbidden transition $^4A_2 \rightarrow {}^2E$. It was established [11–13,17,18] that below the Néel temperature the Davydov splitting of the single-ion $^4A_2 \rightarrow {}^2E$ transition occurs and instead of R_1 and R_2 absorption lines of ruby five sharp lines labeled 1–5 and located, respectively, at 1.7036, 1.7062, 1.7234, 17263, and 1.7322 eV, appear in Cr_2O_3. However, the assignment of these lines is still a controversial subject [13,18].

Symmetry considerations show that there must exist two E excitons and two A_2 excitons labeled by the irreducible representations of the unitary subgroup D_3. By symmetry arguments only E excitons can be observed in axial polarization in absorption. The same is true about measurements of $\alpha_\perp(\omega)$, since vectors of the magnetic and electric dipole moments have similar transformation properties in D_3. Note that relation (4) may be applied equally well for calculating an exciton contribution to the ME tensor $\alpha_{ii}(\omega)$, because the $\mathbf{k} = 0$ point of the Brillouin zone is the extremum point for exciton energy $\mathcal{E}(\mathbf{k})$ in Cr_2O_3 [17] and, consequently, exciton dispersion does not contribute to the ME tensor [2]. It is essential that no new waves appear at exciton resonance if the light propagates along the C_3 axis and, hence, no additional boundary conditions are necessary [19]. For this reason Eq. (3) is applicable in the region of exciton resonance too.

As seen from Fig. 3, in the region of ^2E transition we observe three lines at the positions corresponding to

lines 1, 4, and 5 in [11–13]. A nearly "discontinuous" dispersive character of the rotation in the region of line 1 is due to its narrow linewidth ~5 meV, which is consistent with the absorption data [15]. (We note that lines 1, 4, and 5 were also observed in the optical second harmonic spectrum, however, with a different relative intensity ratio [20].) Lines 1 and 4 were assigned to E excitons and line 5 to exciton-magnon excitation [13]. The conjecture of [18] that line 5 is due to A_2 exciton is now questionable. However, our data cannot be entirely reconciled with the assignments of [13]. First, in [13] line 5 was observed in σ and π, but not in axial polarization. Second, the theory of Frenkel excitons in Cr_2O_3 proposed in [13] gives ellipticities of equals signs for two E excitons, whereas we observe the ellipticities of opposite signs. The analysis of these disagreements is outside the scope of this Letter.

Consider the group of three lines at 1.751, 1.758, and 1.763 eV. It is natural to ascribe these lines to the $^4A_2 \rightarrow {}^2T_1$ transition. Once again we see that the ellipticity spectrum provides much better resolution of the first two lines in these group as compared to the absorption spectrum, in which these lines are broad and weak. The cubic term $^2T_1$ is split by trigonal and exchange fields to components $|a_M \pm \frac{1}{2}\rangle$, where a_M are trigonal components for T_1. The analysis shows [16] that only transitions to $|a_0, -\frac{1}{2}\rangle$ and $|a_+, -\frac{1}{2}\rangle$ components from $|^4A_2, -\frac{3}{2}\rangle$ are allowed. If this simple picture were true, the $^2T_1$ band would give rise to two lines separated from each other by the trigonal field splitting. However, small but clearly defined splitting of 1.751 and 1.758 eV lines (see Fig. 3) makes this explanation invalid. We have tried to reach an agreement with the experiment by taking into account spin-orbit interaction which, combined with the trigonal field, mixes $|a_0, -\frac{1}{2}\rangle$ with $|a_-, \frac{1}{2}\rangle$ and $|a_+, -\frac{1}{2}\rangle$ with $|a_0, \frac{1}{2}\rangle$. The resulting picture depends on the relation between the trigonal and exchange splitting. However, in any case we were unable to obtain a picture similar to that observed experimentally. We may speculate that lines 1.751 and 1.758 eV are due to E excitons associated with transitions to the trigonal term $^2E(^2T_1)$.

Since the product of matrix elements $d_{gn}m_{gn}$ should be proportional to the odd part of the trigonal field v_o, it follows from the above consideration that for spin-allowed d-d transitions the ME tensor $\alpha_\perp(\omega)$ varies as $\lambda_{so}v_o$ (see also [3]), whereas for spin-forbidden d-d transitions $\alpha_\perp(\omega) \sim \lambda_{so}^2 v_o$. The relation between these two values is proportional to λ_{so} unlike the relation between absorption intensities of spin-forbidden and spin-allowed transitions which is proportional to λ_{so}^2 [16].

In conclusion, we have presented a new kind of spectroscopy which gives an alternative approach to a study and analysis of electronic states and can be applied to materials with broken space-inversion and time-reversal symmetries. The nonreciprocal rotation and ellipticity in reflection arise in such crystals due to the electric dipole–magnetic dipole interference for transitions between the same pairs of electronic states. The spontaneous nonreciprocal rotation and ellipticity in reflection are observed in Cr_2O_3. Unlike the well known polar Kerr effect in ferromagnets, which is due to the presence of a magnetic moment, these effects in antiferromagnetic Cr_2O_3 are observed in the absence of any magnetic moment below T_N. Their magnitudes are comparable to those in some ferromagnetic materials. We explain the spectral variations of these effects as arising under a combined action of the trigonal and exchange fields as well as the spin-orbit interaction. Some previous assignments of exciton lines cannot be entirely reconciled with our data and these contradictions require a further theoretical study.

This work was supported in part by the Russian Foundation for Basic Research and by a Grant of the International Science Foundation.

[1] L. D. Baron, *Molecular Light Scattering and Optical Activity* (Cambridge University Press, Cambridge, 1982).
[2] R. M. Hornreich and S. Shtrikman, Phys. Rev. **171**, 1065 (1968).
[3] V. N. Muthukumar, R. Valenť, and C. Gros, Phys. Rev. Lett. **75**, 2766 (1995).
[4] I. Dzyaloshinskii and E. V. Papamichail, Phys. Rev. Lett. **75**, 3004 (1995).
[5] E. B. Graham and R. E. Raab, Philos. Mag. **66**, 269 (1992).
[6] V. M. Agranovich and V. L. Ginzburg, in *Progress in Optics*, edited by E. Wolf (North-Holland, Amsterdam, 1971), Vol. 9, p. 237.
[7] B. B. Krichevtsov, V. V. Pavlov, R. V. Pisarev, and V. N. Gridnev, J. Phys. Condens. Matter **5**, 8233 (1993).
[8] N. I. Zheludev *et al.*, Phys. Rev. B **50**, 11 508 (1994); **52**, 2203 (1995).
[9] L. C. Lew Yan Voon, A. Fainstein, P. Etchegoin, P. Santos, and M. Cardona, Phys. Rev. B **52**, 2201 (1995).
[10] A. L. Shelankov and G. E. Pikus, Phys. Rev. B **46**, 3326 (1992).
[11] K. A. Wickersheim, J. Appl. Phys. **34**, 1224 (1963).
[12] J. P. van der Ziel, Phys. Rev. Lett. **18**, 237 (1967).
[13] J. W. Allen, R. M. Macfarlane, and R. L. White, Phys. Rev. **179**, 523 (1969).
[14] W. A. Crossley, R. W. Cooper, J. L. Page, and R. P. van Stapele, Phys. Rev. **181**, 896 (1969).
[15] D. S. McClure, J. Chem. Phys. **38**, 2289 (1963).
[16] S. Sugano and Y. Tanabe, J. Phys. Soc. Jpn. **13**, 880 (1958).
[17] R. M. Macfarlane and J. W. Allen, Phys. Rev. B **4**, 3054 (1971).
[18] J. W. Allen, Phys. Rev. B **9**, 259 (1974).
[19] V. M. Agranovich and V. L. Ginzburg, *Spatial Dispersion in Crystal Optics and the Theory of Excitons* (Springer-Verlag, Berlin, 1984), 2nd ed.
[20] M. Fiebig, D. Fröhlich, B. B. Krichevtsov, and R. V. Pisarev, Phys. Rev. Lett. **73**, 2127 (1994).